

Bidirectional Perfect Absorber Using Free Substrate Plasmonic Metasurfaces

Jianxiong Li, Ping Yu, Chengchun Tang, Hua Cheng, Junjie Li, Shuqi Chen,* and Jianguo Tian

Much effort has been made to achieve metasurface absorbers with polarization-insensitive, wide-angle, multiband, or broadband performance from gigahertz to terahertz to optical ranges. However, there are well-known challenges in optimizing the performance of metasurface absorbers, due to the existence of a theoretical limit. It is urgent to extend and improve the optical properties of metasurface absorbers to satisfy the requirements for practical applications. Here, a novel free substrate metasurface absorber is demonstrated that has high spatial frequencies on the surface and can prevent light transmission and reflection by transforming free-space incident waves into evanescent waves. Experimental and simulation results show that the proposed metasurface absorber can realize bidirectional perfect absorption and that the absorption of the light incident on one side of the metasurface is independent of the light incident on the other. Hence, the bidirectional perfect absorption does not depend on coherence of the beams. The proposed metasurface provides new degrees of freedom to realize a perfect absorber with twice the absorption capacity. It could have a wide range of applications and profound implications in photodetection, solar light harvesting, and sensing.

Plasmonic metasurfaces are a new class of quasi-2D metamaterials that offer interesting possibilities for manipulating light.^[1,2] A number of fascinating phenomena and applications that challenge our understanding of the electromagnetic response of materials, including negative refraction indices,^[3] invisibility cloaking,^[4–6] controllable optical activity,^[7] and flat lenses that focus light beyond the diffraction limit^[8] have been demonstrated by engineering the geometry of nanostructured metasurfaces. While the high light absorption by plasmonic nanostructures is undesirable for applications requiring high transmittance or reflectivity, it has served to introduce the concept of “metasurface perfect absorbers,” which has increased

the significance of metasurfaces.^[9] Metasurface absorbers have attracted considerable interest and motivated a number of theoretical and experimental studies over the past few years. Many efforts have been made to achieve metasurface absorbers with polarization-insensitive,^[10] wide-angle,^[11] multiband,^[12,13] or broadband performance^[14] from gigahertz to terahertz to optical ranges, which could have many different potential applications. However, the traditional metasurface absorbers exist theoretical limit. The basic idea of the traditional metasurface absorbers is to simultaneously minimize the reflectance through the interference of multiple reflections, eliminate the transmittance through introducing metallic ground on the bottom of metasurface, and maximize the structure losses.^[15] Their electric and magnetic response can be properly tuned by tailoring the structure. Based on this theory, the reported metasurface absorbers have

a lot of limitations in the structural designs, which are often made up of a dielectric spacer sandwiched between resonators and metallic ground plane.^[10–16] Therefore, there are well-known challenges in optimizing the performance of metasurface absorbers, and it is urgent to tackle the barriers posed by the theoretical limit and improve the optical properties of metasurface absorbers to satisfy the requirements for practical applications.

Recently, new degrees of freedom were attained by introducing abrupt phase changes via plasmonic metasurfaces.^[17,18] Such metasurfaces are capable of generating a wide range of position-dependent discontinuous interfacial phase profiles. Since an abrupt phase shift over the wavelength scale can be introduced, the relationship between the incident and refracted beams seems to go beyond the standard Snell's law.^[17] By simply engineering the metasurface-induced phase profile, a nearly arbitrary wavefront can be achieved.^[19–22] This unique approach, viz. introducing an abrupt phase change using a flat metasurface, promises interesting device applications beyond the scope of conventional components that rely on gradual phase accumulation to shape the wavefront. It has already been used to demonstrate some exotic phenomena, including anomalous reflection and refraction,^[17] the spin Hall effect of light,^[23] plasmonic metalens,^[24] metasurface holograms,^[25] optical polarization conversion of light,^[26] and so on. Therefore, controlling the wavefront by using metasurfaces

Dr. J. Li, Dr. P. Yu, Prof. H. Cheng, Prof. S. Chen, Prof. J. Tian
Laboratory of Weak Light Nonlinear Photonics
Ministry of Education
School of Physics and Teda Applied Physics Institute
Nankai University
Tianjin 300071, China
E-mail: schen@nankai.edu.cn

Prof. C. Tang, Prof. J. Li
Beijing National Laboratory for Condensed Matter Physics
Institute of Physics
Chinese Academy of Sciences
P.O. Box 603, Beijing 100190, China

DOI: 10.1002/adom.201700152

offers a new way to manipulate fundamental optical processes such as absorption, emission, and refraction at the nanoscale. It also provides the opportunity to realize novel metasurface absorbers, tackle the barriers posed by theoretical performance limits, and solve current issues in this research field.

In this letter, we present the design, characterization, and experimental demonstration of a novel bidirectional perfect absorber in the near infrared regime. This absorber consists of two pairs of nanoapertures, as opposed to traditional metasurface absorbers with a sandwich configuration. Through a special structural arrangement, a large phase gradient can be generated on the metasurface interface, which leads to the transformation of free-space incident waves into evanescent waves. The experimental and simulation results show that the proposed metasurface absorber can realize bidirectional perfect absorption. Based on special nanofabrication process, proposed metasurface absorber is free substrate, and it has strict symmetry in the z -direction. It means that metasurface absorber has the same absorption peak when the light comes from two sides. Further, the bidirectional perfect absorption of such a metasurface does not depend on the coherence of the beams, and it is retained for any phase difference between the light incident on both sides. The new degrees of freedom enabled by this novel absorber provide twice the absorption capacity in a single metasurface and could have a wide range of applications and profound implications in photodetection, solar light harvesting, and sensing.

Controlling the light wavefront has become an important research subfield of metasurfaces. It offers new degrees of freedom to manipulate fundamental optical properties. It is well known that the propagation direction of light can be easily tuned by generating a special wavefront, and this can be done by simply engineering the arrangement of the nanostructures. The coupling of free-space photons to surface plasmon polaritons (SPPs) can also be easily realized by specially designed metasurfaces. Let us consider a plane wave of unit amplitude traveling in the z -direction, which is transmitted through a metasurface with complex-amplitude transmittance. The transmission process can be described through the following expressions

$$g(x, y, z) = H(v_x, v_y) f(z) = A \exp[-j2\pi(v_x x + v_y y)] \exp(-jk_z z) \quad (1)$$

$$k_z = \sqrt{k^2 - k_x^2 - k_y^2} = 2\pi\sqrt{\lambda^{-2} - v_x^2 - v_y^2}$$

where $f(z)$ and $g(x, y, z)$ are the complex amplitudes of the input and output light, $H(v_x, v_y)$ is the transfer function of the metasurface, k and λ are the wavevector and wavelength of the light, respectively, and $v_x = k_x/2\pi$ and $v_y = k_y/2\pi$ are the spatial frequencies in the x - and y -direction of the metasurface. Therefore, the incident wave is modulated by a harmonic function. For spatial frequencies such that $v_x^2 + v_y^2 < \lambda^{-2}$, the magnitude $|\exp(-jk_z z)| = 1$ and the phase $\arg\{\exp(-jk_z z)\}$ is a function of v_x and v_y . The incident wave is then converted into a plane wave with a wavevector whose direction is given by the angles $\theta_x = \sin^{-1} \lambda v_x$ and $\theta_y = \sin^{-1} \lambda v_y$, and whose magnitude is not altered. At higher spatial frequencies, $v_x^2 + v_y^2 > \lambda^{-2}$, the quantity under the square root in Equation (1) becomes negative, so the exponent is real and $\exp(-jk_z z)$ represents an attenuation factor. The output wave is an evanescent wave, whose magnitude

will decay exponentially. In this case, the free-space incident wave is totally transformed into SPPs, whence the transmittance is zero.^[27] Therefore, we can achieve vanishing transmittance and reflectance by inducing a large phase gradient on the metasurface, corresponding to high spatial frequencies ($v_x^2 + v_y^2 > \lambda^{-2}$). This provides the opportunity to realize a novel metasurface absorber by shaping the light wavefront, which requires designing a kind of nanostructures that allow us to control the phase of the transmitted and reflected light.

The unit cells of the proposed metasurfaces with rectangular nanoapertures are schematically shown in **Figure 1a,b**. Two gold layers with 70 nm thick are separated by a layer of dielectric with 70 nm thick along the z -axis. The top and bottom nanoapertures are either aligned or separated by a distance S along the y -direction. The optical parameters of gold are described using the Drude model.^[28] The whole structure is embedded in silicon nitride, whose dielectric constant is 4. We performed numerical simulations using a 3D finite element method with COMSOL Multiphysics.^[29] SPPs can be apparently excited at the metal–dielectric interfaces by the normally incident light polarized along the y -direction. A standing wave of SPPs can be formed because of the coupling between two metal layers. A metal–insulator–metal (MIM) waveguide can therefore be obtained (see **Figure 1e**), where the phase and amplitude of the transmitted light are sensitive to the dimensions and geometry. For example, we can obtain a wide range of phase shifts by tuning the aperture length L in the aligned case $S = 0$. Due to the excitation of surface waves and localized resonance, a high transmission amplitude can be maintained across a wide range of L . The range of phase shifts can be further extended by tuning the lateral translation S between the top and bottom nanoapertures. The calculated phase of the transmitted light from the plasmonic metasurfaces as a function of the aperture lateral translation S is shown in **Figure 1f**. Two out-coupling maxima can be found at $S = 0$ and $S = P/2$. Since the strongest charge oscillation can be established within the bottom individual nanoapertures, the efficient dipole radiation in the transmission direction can be realized. Furthermore, the transmitted phase difference for these two conditions is close to π (see **Figure 1c,d**). The reason is that the charge oscillations at the bottom nanoapertures have opposite directions.^[22]

In order to experimentally validate the bidirectional metasurface perfect absorber described above, we use two pairs of nanoapertures to form a super-unit-cell in **Figure 2a**. The proposed metasurfaces consisting of a periodic array of individual subunits have similar transmission amplitudes and a transmitted phase difference of π at the designed wavelength. In this way, a constant large phase gradient along the metasurface can be created to transform free-space incident waves into evanescent waves. It should be emphasized that the super-unit-cell has strict symmetry in the z -direction, which means that the reflection and absorption spectra do not depend on which side is illuminated by the incident light. **Figure 2b** shows scanning electron microscopy (SEM) images of the metasurface structure, which was fabricated by sputtering deposition of gold and Si_3N_4 , electron-beam lithography, and reactive ion etching.^[22] In order to obtain strict structural symmetry in the z -direction, an Au nanostructure was deposited onto the self-supporting Si_3N_4 film. A 200 nm thick polymethyl methacrylate (PMMA)

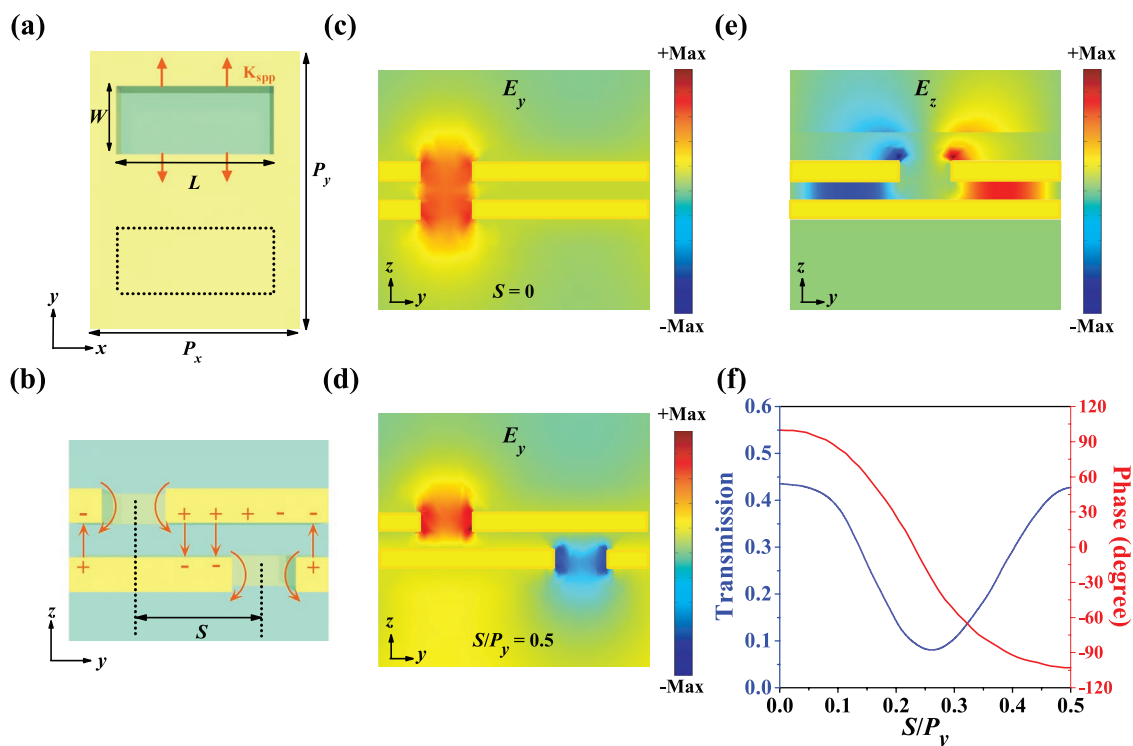


Figure 1. Schematic illustration of the unit cells: a) top view and b) lateral view. The rectangular nanoapertures in the two layers have the same dimensions. The surface plasmonic standing wave is shown between the two metallic structures, with the charge oscillation indicated. The rectangular with dotted line represent the position of the nanoaperture in the bottom layer. c,d) Simulated E_y patterns for the aligned and translated nanoapertures in the yz plane, with periods $P_x = 455$ nm and $P_y = 1000$ nm, $L = 305$ nm and $W = 195$ nm. e) Simulated E_z patterns of an MIM waveguide with periodic rectangular nanoapertures in the top metal film in the yz plane. f) Calculated phase of the transmitted light from the plasmonic metasurfaces as a function of the aperture lateral translation S , for a structure with aperture length $L = 305$ nm and width $W = 195$ nm.

resist was subsequently spin coated onto the sample, which was then subjected to bake out on a hotplate at 180 °C for 2 min. The pattern was exposed using an electron-beam lithography

system (Raith150, Raith GmbH, Dortmund, Germany) at 10 keV. After the exposure, the sample was developed in methyl isobutyl ketone:isopropyl alcohol (MIBK:IPA) (1:3) for 40 s and IPA for 30 s and then blown dry with pure nitrogen. The pattern was transferred onto the Au layer by a reactive-ion etching system using Ar gas. After removing the PMMA resist with acetone, a 70 nm thick Si_3N_4 layer was deposited onto the sample using plasma-enhanced chemical vapor deposition (PECVD). The pattern on the second Au layer was prepared by repeating the exposure, etching, and resist-removal processes. Finally, a 70 nm thick SiO_2 layer was deposited on the top of the sample using PECVD.

We used a Fourier-transform IR spectrometer (VERTEX 70, Bruker Optics, Ettlingen, Germany) to measure the reflection and transmission spectra of the sample, from which the absorption spectrum can be calculated. Those spectra were recorded by averaging the data from 64 measurements, in order to improve the signal-to-noise ratio. The simulated and experimental absorption spectra of the designed structures are shown in Figure 3. When the incident light illuminates the front of the metasurface, the

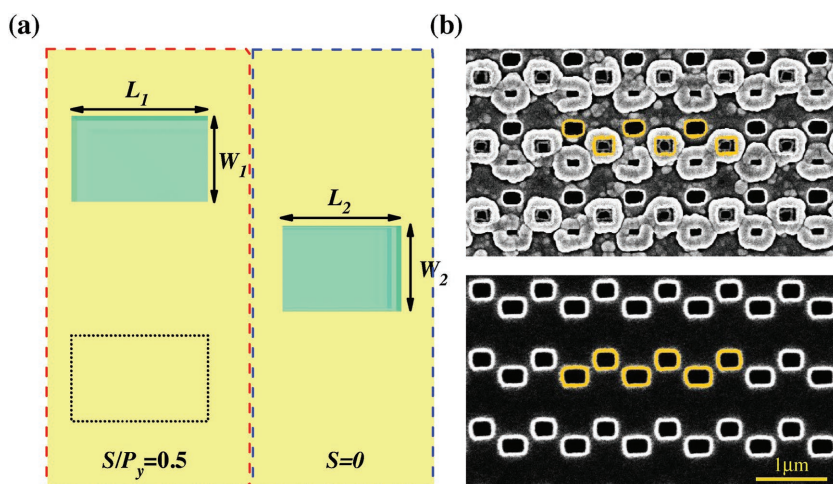


Figure 2. a) Schematics of the nanoapertures forming the super-unit-cell in the plasmonic metasurface absorber. The optimized geometrical parameters of the nanoapertures are $L_1 = 305$ nm, $L_2 = 320$ nm, and $W_1 = W_2 = 195$ nm. The dimensions of the subunits in the y - and x -direction are 1000 and 875 nm, respectively, while the lateral translation S is 0 and 500 nm, respectively. b) SEM images of a fabricated plasmonic metasurface after finishing the first layer (lower panel) and after complete fabrication (upper panel). The super-unit-cell in each layer is highlighted in yellow.

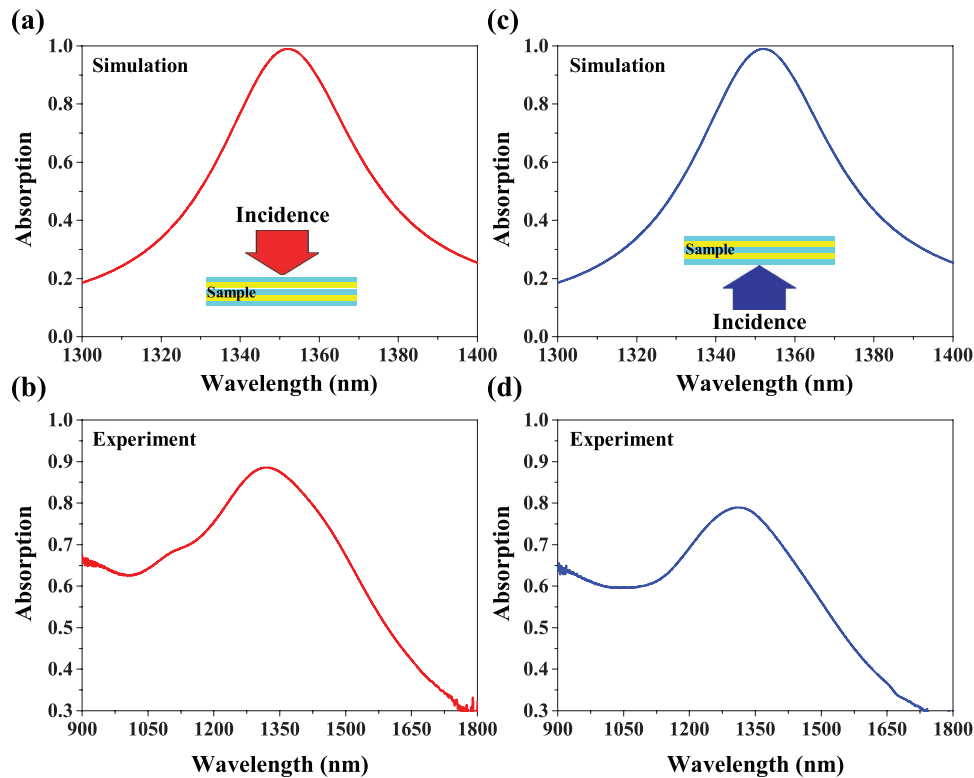


Figure 3. a) Simulated and b) experimental absorption spectra of the sample when the incident light illuminates the front side. (c) and (d) are analogous figures for incident light illuminating the back side.

simulation results show perfect absorption at a wavelength of 1352 nm. Due to the symmetry of the nanostructures, the absorption spectrum is identical for incident light reaching the back of the absorber. The experimental results also show significant absorption, in good agreement with the simulation. The absorption is about 88% and 79% for incident light reaching the front and back of the metasurface, respectively. The discrepancy between the simulation and the experimental results should be mainly caused by the inevitable structural imperfections of the fabricated sample shown in Figure 2b. The experimental results show that the sample exhibits bidirectional absorption, a totally different behavior from that of traditional absorbers.

To better understand the nature of this novel metasurface absorber, we investigated the amplitude and direction of the electric field through numerical simulation. Figure 4a,b shows the electric field direction (white arrows) and amplitude distribution (colormaps) on the back and front side of the metasurface at the absorption peak, when the incident light illuminates the front side of the absorber. On the other hand, Figure 4c,d shows the cross-line value of the electric field phase as a function of the x -axis position on the surface shown in Figure 4a,b. We find that the two fabricated nanoaperture structures have indeed similar transmission amplitudes and a phase difference of π in the transmitted electric field at the absorption wavelength. Therefore, two nanoapertures with a periodic arrangement form a large phase gradient on the interface of the metasurface. The period of the unit cell is 1000 nm, and the spatial frequency ν_y in the y -direction is about 10^6 Hz, which satisfies the relationship $\nu_y^2 > \lambda^{-2}$ at the absorption wavelength

of 1352 nm. Thus, the output wave will be an evanescent wave, according to Equation (1), and its magnitude will decay exponentially. In these conditions, the free-space incident wave is totally transformed into SPPs, and the transmittance is zero. The situation for the electric field reflected by the metasurface is similar. Figure 4b,d shows that the electric field in the zones with and without nanoaperture structures also has similar transmission amplitude and opposite resonance direction at the absorption wavelength. Therefore, a large phase gradient and high spatial frequencies ν_y in the y -direction, satisfying the relationship $\nu_y^2 > \lambda^{-2}$, are formed on the interface of metasurface. Thus, the reflected wave is again an evanescent wave, and the reflectivity is zero. The basic idea behind traditional metasurface absorbers is to simultaneously minimize the reflectance through the interference of multiple reflections, eliminate the transmittance using a metallic ground plane, and maximize the structure losses. However, the novel metasurface absorber proposed here depends on the transformation of free-space incident waves into evanescent waves to eliminate the reflectance and transmittance, according to the phase control provided by the nanoaperture structures. It behaves as a bidirectional perfect absorber, which can double the absorption capacity of a single metasurface. Therefore, this novel metasurface absorber tackles the barriers posed by the theoretical performance limit and overcomes the limitations of sandwich nanostructures, largely expanding and improving the optical properties of metasurface absorbers.

It is obvious that the symmetry of the metasurface in the z -direction plays an important role in bidirectional absorption. At the same time, the absorption of the light incident on the

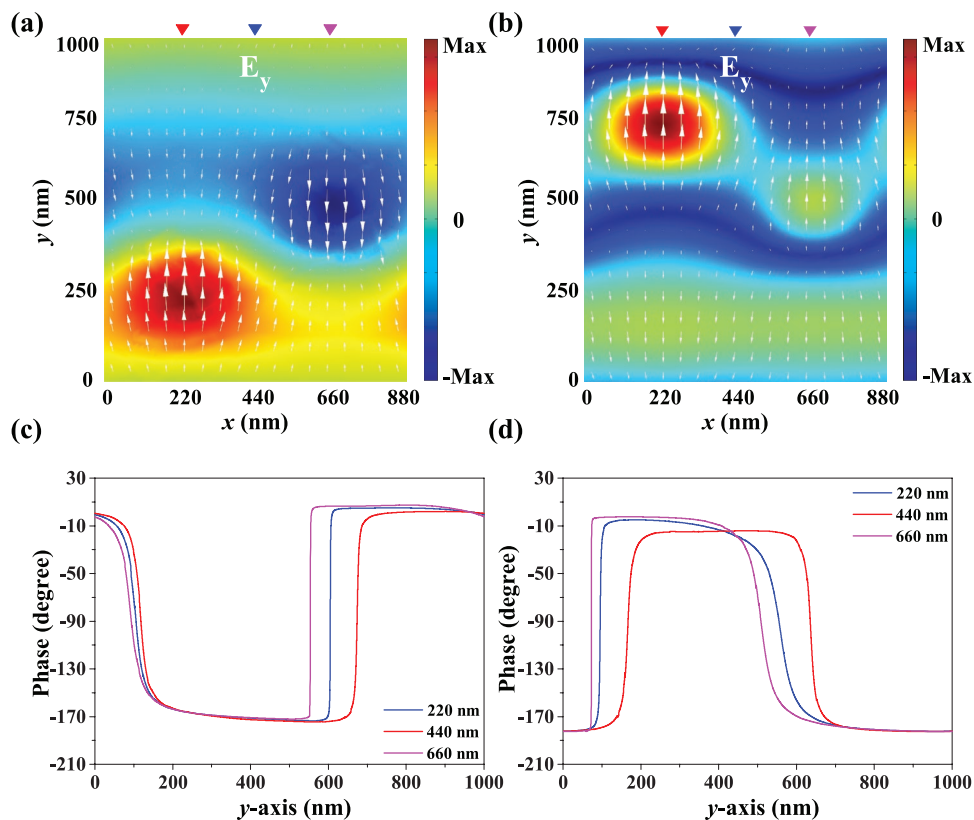


Figure 4. Simulated electric field direction (white arrows) and amplitude distribution (colormaps) on a) the back and b) front side, at the absorption peak and when the incident light illuminates the front of the metasurface; (c) and (d) show the cross-line value of the electric field phase as a function of the x -axis position in c) the back and d) front side at the absorption peak.

front of the absorber is independent of the light reaching its back. Therefore it is possible that the proposed metasurface could simultaneously absorb incident light illuminating both sides. **Figure 5a** shows the output intensity of the metasurface, defined as the sum of all the transmitted and reflected intensity when the incident light simultaneously illuminates both sides. If the output intensity is zero, that means that all the incident light (on both sides) is absorbed by the metasurface. This is precisely what the simulation results show at 1352 nm;

see **Figure 5a**. Recently, coherent perfect absorbers have drawn significant attention from researchers because of their unique electromagnetic properties.^[30] A coherent perfect absorber can achieve complete absorption at a single frequency by sending two counterpropagating fields to a Fabry–Perot cavity that possesses a lossy slab. Coherent perfect absorbers have vast applications in interferometry procedures in optical circuits and technologies related to light harvesting. However, they need coherent illumination by two beams, and the phase difference

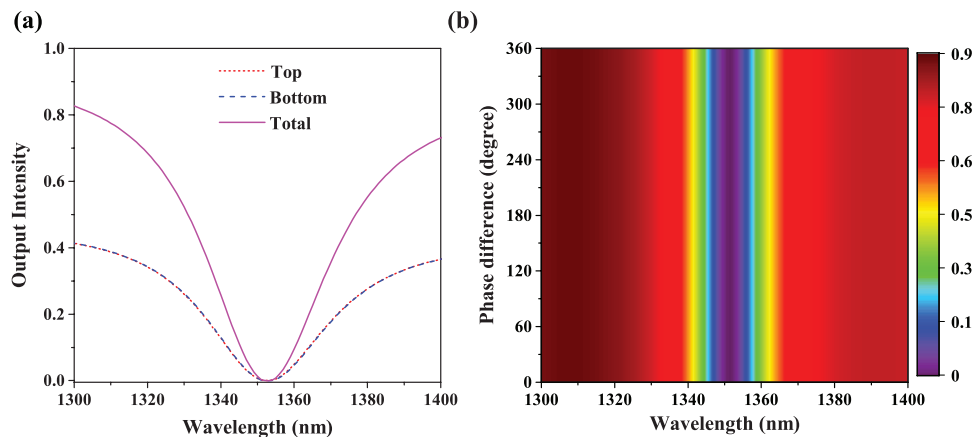


Figure 5. a) Simulated output intensity spectrum of the proposed metasurface, when the incident light simultaneously illuminates both sides. b) Simulated output intensity spectrum as a function of the phase difference between the incident light that illuminates both sides.

between these has a great impact on the absorption capacity of the materials. In particular, bidirectional perfect absorption occurs only for a certain phase difference. However, for many practical applications it is desirable to achieve bidirectional perfect absorption when using incoherent beams, a characteristic of the novel metasurface absorber presented here. In order to prove that the absorption of the light illuminating the front side of the metasurface is independent of the light illuminating its back, we obtain the output intensity spectrum as a function of the phase difference between those two beams; see Figure 5b. We observe that the proposed metasurface maintains bidirectional perfect absorption for any phase difference between 0 and 2π . Therefore, the proposed metasurface is quite different from coherent absorbers, as it has the unique characteristic of independent bidirectional perfect absorption. Our results open a new avenue for designing new types of absorbers and sensors, which can double the absorption capacity of a single metasurface.

In summary, we have proposed and experimentally validated a novel metasurface absorber that exhibits bidirectional perfect absorption, based on the manipulation of the light phase. Through a special structural arrangement, a large phase gradient can be generated on the metasurface interface, which leads to the transformation of free-space incident waves into evanescent waves. This way of eliminating the transmittance and reflectance is different from the method used by traditional absorbers with a sandwich configuration and also from that employed by coherent perfect absorbers. The proposed metasurface absorber can realize simultaneously bidirectional perfect absorption, and the absorption of the light incident on one side is independent of the light that illuminates the other. Simulation results show that the proposed metasurface absorber maintains bidirectional perfect absorption for any phase difference between 0 and 2π . Therefore, the proposed perfect absorber can double the absorption capacity of a single metasurface, and tackles the barriers posed by the theoretical performance limit and overcomes the limitations of sandwich nanostructures, largely expanding and improving the optical properties of metasurface absorbers. The demonstration is in the near infrared wavelength range, but the approach of realizing bidirectional perfect absorption can be easily translated to mid-infrared, terahertz, and microwave frequency regimes. Therefore, the novel metasurface absorber tackles the barriers posed by the theoretical performance limit, largely expanding and improving the optical properties of metasurface absorbers. As a result, it could find numerous applications, ranging from detection to sensing.

Acknowledgements

This work was supported by the National Key Research and Development Program of China (2016YFA0301102), the Natural Science Foundation of China (11574163 and 61378006), the Program for New Century Excellent Talents in University (NCET-13-0294), and the 111 project (B07013). The authors also acknowledge the support from the Collaborative Innovation Center of Extreme Optics, Shanxi University, Taiyuan, Shanxi 030006, China.

Conflict of Interest

The authors declare no conflict of interest.

Keywords

absorbers, metasurfaces, plasmonics

Received: February 16, 2017

Revised: March 24, 2017

Published online:

- [1] N. Yu, F. Capasso, *Nat. Mater.* **2014**, *13*, 139.
- [2] H. Cheng, Z. Liu, S. Chen, J. Tian, *Adv. Mater.* **2015**, *27*, 5410.
- [3] R. A. Shelby, D. R. Smith, S. Schultz, *Science* **2001**, *292*, 77.
- [4] F. Zhou, Y. Bao, W. Cao, C. T. Stuart, J. Gu, W. Zhang, C. Sun, *Sci. Rep.* **2011**, *1*, 78.
- [5] D. Liang, J. Gu, J. Han, Y. Yang, S. Zhang, W. Zhang, *Adv. Mater.* **2012**, *24*, 916.
- [6] X. Chen, Y. Luo, J. Zhang, K. Jiang, J. B. Pendry, S. Zhang, *Nat. Commun.* **2011**, *2*, 176.
- [7] P. Yu, J. Li, C. Tang, H. Cheng, Z. Liu, Z. Li, Z. Liu, C. Gu, J. Li, S. Chen, J. Tian, *Light: Sci. Appl.* **2016**, *5*, e16096.
- [8] J. B. Pendry, *Phys. Rev. Lett.* **2000**, *85*, 3966.
- [9] C. M. Watts, X. Liu, W. J. Padilla, *Adv. Mater.* **2012**, *24*, OP98.
- [10] K. Aydin, V. E. Ferry, R. M. Briggs, H. A. Atwater, *Nat. Commun.* **2011**, *2*, 517.
- [11] X. Duan, S. Chen, W. Liu, H. Cheng, Z. Li, J. Tian, *J. Opt.* **2014**, *16*, 125107.
- [12] H. Cheng, S. Chen, H. Yang, J. Li, X. An, C. Gu, J. Tian, *J. Opt.* **2012**, *14*, 085102.
- [13] Y. Ma, Q. Chen, J. Grant, S. C. Saha, A. Khalid, D. R. S. Cumming, *Opt. Lett.* **2011**, *36*, 945.
- [14] S. Chen, H. Cheng, H. Yang, J. Li, X. Duan, C. Gu, J. Tian, *Appl. Phys. Lett.* **2011**, *99*, 253104.
- [15] N. Liu, M. Mesch, T. Weiss, M. Hentschel, H. Giessen, *Nano Lett.* **2010**, *10*, 2342.
- [16] H. Chen, *Opt. Express* **2012**, *20*, 7165.
- [17] N. Yu, P. Genevet, M. A. Kats, F. Aieta, J. Tetienne, F. Capasso, Z. Gaburro, *Science* **2011**, *334*, 333.
- [18] X. Zhang, Z. Tian, W. Yue, J. Gu, S. Zhang, J. Han, W. Zhang, *Adv. Mater.* **2013**, *25*, 4567.
- [19] X. Ni, A. V. Kildishev, V. M. Shalaev, *Nat. Commun.* **2013**, *4*, 2807.
- [20] X. Chen, L. Huang, H. Mühlenbernd, G. Li, B. Bai, Q. Tan, G. Jin, C. Qiu, S. Zhang, T. Zentgraf, *Nat. Commun.* **2012**, *3*, 1198.
- [21] N. Yu, F. Aieta, P. Genevet, M. A. Kats, Z. Gaburro, F. Capasso, *Nano Lett.* **2012**, *12*, 6328.
- [22] J. Li, S. Chen, H. Yang, J. Li, P. Yu, H. Cheng, C. Gu, H.-T. Chen, J. Tian, *Adv. Funct. Mater.* **2015**, *25*, 704.
- [23] X. Yin, Z. Ye, J. Rho, Y. Wang, X. Zhang, *Science* **2013**, *339*, 1405.
- [24] A. Pors, M. G. Nielsen, R. L. Eriksen, S. I. Bozhevolnyi, *Nano Lett.* **2013**, *13*, 829.
- [25] L. Huang, X. Chen, H. Mühlenbernd, H. Zhang, S. Chen, B. Bai, Q. Tan, G. Jin, K. W. Cheah, C. W. Qiu, J. Li, T. Zentgraf, S. Zhang, *Nat. Commun.* **2013**, *4*, 2808.
- [26] N. K. Grady, J. E. Heyes, D. R. Chowdhury, Y. Zeng, M. T. Reiten, A. K. Azad, A. J. Taylor, D. A. Dalvit, H. T. Chen, *Science* **2013**, *340*, 1304.
- [27] L. Huang, X. Chen, B. Bai, Q. Tan, G. Jin, T. Zentgraf, S. Zhang, *Light: Sci. Appl.* **2013**, *2*, e70.
- [28] E. D. Palik, *Handbook of Optical Constants of Solids*, Academic Press, San Diego, CA, USA **1998**.
- [29] COMSOL Multiphysics, Version 3.5, Comsol AB, Brulington, MA, USA **2008**.
- [30] W. Wan, Y. Chong, L. Ge, H. Noh, A. D. Stone, H. Cao, *Science* **2011**, *331*, 889.